Building and Environment 49 (2012) 9–16

Contents lists available at SciVerse ScienceDirect

Building and Environment

journal homepage: www.elsevier.com/locate/buildenv

An optoelectronic sensor for the monitoring of mould growth in concealed spaces

Eric Savory[a,*], Jayshri Sabarinathan[b], Anna Sauer[b], James A. Scott[c,d]

[a] Department of Mechanical and Materials Engineering, University of Western Ontario, 1151 Richmond Street, London, Ontario N6A 5B9, Canada
[b] Department of Electrical and Computer Engineering, University of Western Ontario, 1151 Richmond Street, London, Ontario N6A 5B9, Canada
[c] Dalla Lana School of Public Health, University of Toronto, 223 College Street, Toronto, Ontario M5T 1R4, Canada
[d] Sporometrics Inc., 219 Dufferin St Suite 20-C, Toronto, Ontario M6K 1Y9, Canada

ARTICLE INFO

Article history:
Received 28 June 2011
Received in revised form
19 September 2011
Accepted 20 September 2011

Keywords:
Optoelectronics
Sensor
Mould
Monitoring
Building envelope
Healthy housing

ABSTRACT

The growth of mould in the indoor environment is an important contributor to the development and exacerbation of atopic disease, and potentially poses other health risks. Moreover, the detection and elimination of mould have resulted in massive remedial expenditures, often without clear engineering knowledge of the nature of the moisture events that led to the damage, especially for residential light wood-frame construction. Relatively little research has considered such failure of the building enclosure as a starting point for developing practical, evidence-based construction practices to improve building performance. One research limitation concerns the use of invasive or destructive testing as the sole means to monitor mould growth in concealed assemblies, such as wall cavities, making it difficult or impossible to conduct time-course experiments to assess the performance of different materials and designs. The present paper concerns the development and testing of a new optoelectronic sensor capable of non-invasive monitoring of mould growth in concealed spaces in real-time by measuring changes in light reflectance from the sensor's active element, a membrane impregnated with mould spores. It builds upon an earlier concept [1] in which mould-impregnated cellophane coupons were attached to building surfaces, then removed and examined periodically for growth by microscopy. The new device incorporates computer-controlled measurement of mould growth, in response to the environmental conditions and, thus, functions as a remote sensor. Although primarily intended for research use, the device has the potential to be used as a post-remediation monitoring device to provide early-warning of any re-occurrence of mould growth.

1. Introduction

Indoor mould has long been recognized to pose a risk to human health, particularly in the development and exacerbation of allergy and asthma [2]. From a population health standpoint, indoor mould is increasingly viewed as an important health-relevant exposure in residential housing [3].

Without exception, the growth of mould in the built environment is always mediated by superfluous moisture. In the most straight-forward of situations, moisture can be introduced through catastrophic failure of the building enclosure (i.e., building envelope), as was the case with homes in areas of the southeastern US affected by Hurricane Katrina in 2005. By contrast, far more subtle forms of water incursion are responsible for the vast majority of mould damage in housing. While these may relate to failures of mechanical systems, such as plumbing leaks, or egregious conditions of use and lifestyle, most are the result of relatively minor failures of the building enclosure, manifesting either as breaches that permit the direct penetration of water (e.g., cracked caulking joints, damaged flashing, etc.), or as inadequate thermal management (e.g., thermal bridges produced by framing materials or mechanical penetrations, insufficient insulation, gaps in caulking seals or vapour retarding membranes, etc.), resulting in the inappropriate accumulation of moisture by adsorption and condensation. In some cases, design failures arising from efforts to improve energy efficiency have had the unintended effect of trapping moisture. Regardless of the moisture source, once wetted, most organically-based building materials rapidly become colonized with mould in varying degrees according to their susceptibility.

Some aspects of the indoor mould problem have received considerable attention. In particular, there has been much study of mould-related health effects from both epidemiological and pathophysiological perspectives (reviewed in Refs. [3–5]). Likewise, there exists a growing body of literature on methods and approaches to the investigation of buildings and their remediation

* Corresponding author. Tel.: +1 519 661 2111x88256; fax: +1 519 661 3020.
E-mail address: esavory@eng.uwo.ca (E. Savory).

0360-1323/$ – see front matter © 2011 Elsevier Ltd. All rights reserved.
doi:10.1016/j.buildenv.2011.09.023

(reviewed in Refs. [6,7]). However, there has been relatively little parallel effort to advance the understanding of the contribution of construction practices, architectural and design and building materials to the susceptibility of buildings to mould. These knowledge gaps have been reinforced, in part, by the historical reliance of the construction industry on codes of practice derived from received wisdom and intuition rather than objective evidence. This trend has become further entrenched by the many challenges presented by the study of mould in relation to construction. For example, air and moisture leakage through the building enclosure is rarely a straight-forward phenomenon and cannot easily be adequately modelled using partial wall assemblies. As a further complication, while it is possible to measure temperature, air leakage and moisture in concealed spaces by non-invasive techniques, the evaluation of mould growth typically requires invasive sampling, such as periodic inspection through introduced penetrations, or destructive sampling in which the mould condition is only evaluated at the conclusion of an experiment. Although invasive sampling has the advantage of allowing for the assessment of growth over time in relation to other measured factors, it does so at the risk of modifying the growth conditions themselves.

Non-invasive monitoring of mould growth in concealed spaces has been attempted with mixed success using radar [8]. However, a promising biosensor was developed using mould itself as a proxy [1]. Spores of *Eurotium herbariorum* (chosen because this species grows under a wide range of moisture conditions), together with nutrients, were placed on a piece of undeveloped and fixed, vapour-permeable photographic film. This was covered with a second segment of film (to prevent the inocula from dispersing into the test environment) and placed in a 35 mm photographic slide holder. Each slide could then be affixed to a test surface and removed at periodic intervals for visual and microscopic assessment of growth. Using this device in an apartment building [9], they derived a numerical "fungal index", defined as the sensor's response as a function of exposure time. The response of this index showed strong agreement with temperature and relative humidity measurements (correlation coefficient $= 0.91$, $p = 0.01$) [10].

Although inexpensive and elegant in its simplicity, Abe's "fungus detector" [1] has several drawbacks. Firstly, the slides must be manually removed from the test environment, examined and then replaced. Secondly, where the positioning of the sensors does not coincide with natural openings, artificial penetrations must be introduced, potentially altering the microenvironmental conditions. The reliance on manual observation is labour-intensive, introduces the potential for subjectivity, and provides data only at selected time-points.

To overcome these deficiencies, the present work has adapted Abe's concept by developing a remote sensor. The new sensor consists of a permeable, hydrophilic membrane inoculated with mould spores that is affixed to a test surface over which a miniaturized optoelectronic illumination and sensing device is positioned (Fig. 1). The reflectance characteristics of the membrane can then be measured at user-defined intervals to determine the time of onset of mould growth. Multiple sensors can be embedded in a wall at pre-selected positions during construction. These sensors can then be monitored remotely over time without the need for manual intervention.

The initial prototype development work was presented previously [11]. Here the final version of the sensor is described, together with details concerning its operation and performance and results from laboratory bench-tests and in-wall installations in a test building. It should be noted that the sensor components were chosen to be as inexpensive as possible in order to allow economic construction of multiple sensors.

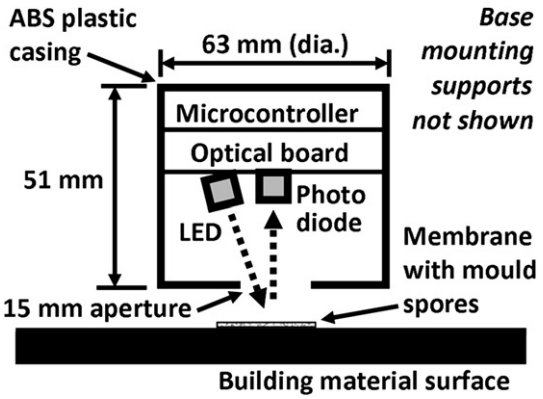

Fig. 1. Conceptual drawing of the sensor.

2. Materials and methods

2.1. Preparation of mould-inoculated membranes

The active element of the device consists of a 25 mm diameter, 0.8 μm pore-size mixed cellulose esters membrane (MCEM, Millipore, Billerica, Massachusetts) inoculated with spores of *Cladosporium sphaerospermum*. This species was selected because it is a common indoor environmental contaminant occurring on a range of materials under relatively low water-activity conditions as a consequence of leakage or condensation. Also, its cells are highly melanized, facilitating the monitoring of its growth by light reflectance [12].

C. sphaerospermum was grown for 7–14 days at room temperature on modified Leonian's agar medium [13]. At the end of this period the Petri plates were flooded with sterile distilled water, and the colony surfaces were gently scraped using a sterile disposable 10 μL bacteriological loop. The suspension was filtered through multiple layers of sterile cheesecloth in a thistle tube funnel to remove large mycelial fragments. The concentration of the resulting spore suspension was enumerated using a haemocytometer and adjusted to approximately 200 cells mL^{-1} by the addition of sterile distilled water. From this stock, a spore suspension was prepared by adding 3500 spores to a sterile broth consisting of 0.8% peptone, 2.5 mM glucose, 5.0 mM NH_4NO_3, 1.6 μM $CuSO_4 \cdot 5H_2O$ and 32.0 μM $ZnSO_4 \cdot 7H_2O$ in distilled water in a total volume of 50 mL. Each suspension was mixed by vortexing and applied immediately to an MCEM aseptically by vacuum filtration. Membranes prepared in this manner were dried aseptically under ambient conditions and stored in darkness until use.

During the development phase of this work, sterilized birch tongue depressors were used to simulate test surfaces. Membranes were adhered to the tongue depressor using an adhesive consisting of sterile molten 2% agarose. The tongue depressors were inserted in sterile 50 mL conical bottom centrifuge tubes into which 2–3 mL of sterile water had been placed, such that the wood was not in direct contact with the water. A series of membranes were prepared in this manner and incubated under ambient conditions for 8 days. Membranes were harvested at 1-day intervals and dried to arrest further growth. An uninoculated membrane treated only with nutrient solution was used as a negative control.

2.2. Optical components

Prior to the selection of a light source, the reflectance characteristics of the set of test membranes described above were evaluated. These assays were conducted using a white LED, placed so its

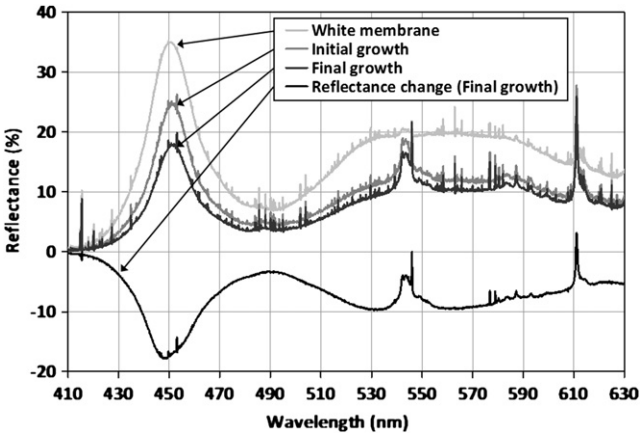

Fig. 2. The normalized spectral response for a mould-covered membrane using a white LED source.

beam covered the entire membrane surface, and a WaveStar Spectrometer (Ophir Photonics Group, Logan, Utah) placed so as to detect the reflected light. Both the LED and the spectrometer were placed at the same angle to the membrane. Maximum absorbance was found to occur between 430 and 470 nm (Fig. 2). Thus, a white or blue LED was deemed to be suitable.

The selection of the light source took into consideration the following performance requirements: low power consumption, uniformity of light intensity across the beam area, beam width, wavelength spectrum of the light output, overall size and cost per unit. The L935NPWC (American Opto Plus LED, Pamona, California) was selected because of its fairly broad constant illumination range, with the output intensity at an illumination angle of 22° still being 94% of that when illuminating normally (that is, at 0° relative to the output axis of the LED).

Despite the relative advantages of using a phototransistor (e.g., no requirement for signal amplification), phototransistors with good sensitivity in the blue spectral region were either of limited availability or prohibitively expensive. Therefore, a TSLB257 (blue filter) photodiode (Texas Advanced Optoelectronic Solutions (TAOS), Plano, Texas) was chosen to serve as the detector.

The normalized responses of the LED and photodiode with respect to angular position were assessed (Fig. 3) as a preliminary

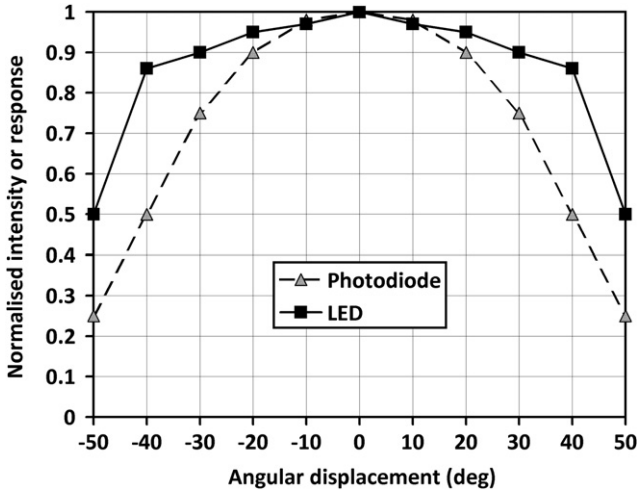

Fig. 3. Angular displacement vs normalized response for the LED and photodiode (re-graphed from datasheets).

step to optimize their positioning so that the photodiode was exposed to the maximum reflection of light from the membrane. Because the photodiode had the poorest angular response of the two devices, it was placed centrally on the optical circuit board in the normal position relative to the membrane. The LED was then located radially to the photodiode and fixed at an angle of 22° towards the photodiode.

2.3. Control unit

The control unit, installed on the second circuit board stacked on top of the optical board, comprised a microcontroller chip (48-pin Motorola MC9S12C32, ON Semiconductor, Phoenix, Arizona), together with a voltage regulator and oscillator. The microcontroller controls the optical board, retrieves data from the optical components, performs analogue-to-digital (A/D) data conversion, and transmits the data via an RS232 connection. Because the microcontroller is unable to provide the 20 mA current required to operate the optical components a transistor was incorporated, with its collector connected to the main power supply and base connected to the microcontroller. The microcontroller provides a 10-bit A/D conversion of the photodiode output voltage, giving a resolution of 4.88 mV step^{-1}.

All of the circuits are powered at 5 V DC, controlled by a voltage regulator (LP2980AIM5-5.0, National Semiconductor, Santa Clara, California) that can accept an input voltage between 5 and 12 V, thereby allowing the sensor to operate using either a direct power source or battery.

Although the selected microcontroller has an internal oscillator that serves as a control clock for its internal functions, it was found that the frequency of this clock was not stable and varied between chips. Hence, it was decided to use an external oscillator (16 MHz, single ASV series chip format, Abracon Corporation, Rancho Santa Margarita, California) in each sensor in order to ensure a consistent timing amongst all the sensors. This is helpful for timing the on/off periods for the LED, sequencing of the DAQ operations and, most importantly, for controlling any future wireless transmission and receiving circuit where timing becomes crucial.

2.4. Communication unit

Data transfer to/from a PC was accomplished by serial communication, incorporating connections to allow for future wireless communication. Serial communication protocol requires data to be transmitted and read in the range of ±10 V. Because the microcontroller reads and writes data in the 0–5 V range, a serial communication chip was incorporated to convert the data leaving and entering the microcontroller (MAX232CWE, Maxin Integrated Products, Sunnyvale, CA). This chip is able to reliably transmit data up to 50 m at 9600 Baud, which is a sufficiently large range to support the current field test installation where the greatest distance between any sensor and the DAQ system is approximately 30 m. In the sensor configuration, the MAX232 chip was not wired directly to the microcontroller; rather, two jumpers were used so that the data could easily be directed to a third circuit board in anticipation of future wireless operation. For the current tests, the jumpers were set to allow the data to be transmitted directly to the MAX232 chip.

2.5. Housing unit

The sensor housing was designed to optimize five criteria: 1) to allow moisture to reach the membrane; 2) to allow the sensor's active space to remain at the ambient environmental conditions; 3) to contain all of the electronic components and batteries with room

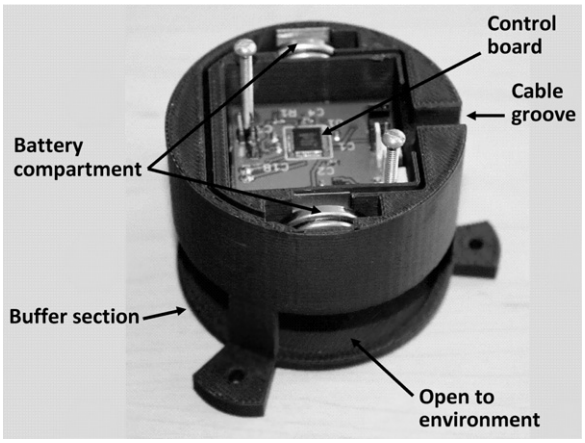

Fig. 4. Side view of the sensor housing unit (without lid).

for the future inclusion of a wireless communications board; 4) to firmly hold the optical components in position; and, 5) to provide shielding from ambient light. A 51 mm (height) × 63 mm (diameter) cylindrical housing was fabricated from black ABS plastic (using a Stratasys in-office rapid prototyping machine) with an interior volume of 38 × 38 × 38 mm to accommodate up to three horizontal electronic circuit boards (Fig. 4). Two 6.3 mm deep slots around the edge of the sensor were included to accept two 25 mm diameter batteries in a configuration that allowed the two batteries to be connected in series, thus providing 6 V supply to the main circuit board. The base of the housing included a 3-point mounting structure and a centrally placed annulus intended to occlude areas of the test surface adjacent to the edges of the membrane [12]; otherwise the lower portion of the housing was kept open to permit the circulation of air and moisture.

2.6. Software

An independent data acquisition system (CR1000 DAQ, Campbell Scientific, Logan, Utah) was used to capture digital data from the sensors, along with analogue data from other environmental monitoring devices for temperature, relative humidity and moisture content. The communication protocol between the microcontroller on each mould sensor and the DAQ used the following general algorithm:

- The microcontroller and the DAQ initiate individual serial communication;
- The microcontroller is set to sleep mode awaiting a wake-up code from the DAQ;
- After sending the wake-up code, the DAQ waits for data to be received from the sensor;
- The sensor checks to ensure the initiation code was correct and proceeds accordingly;
- The sensor switches on, powering the optical board;
- The DAQ delays for a specified amount of time to allow components to stabilize (2 s);
- The sensor awaits a second initiation code from the DAQ;
- Once the DAQ sends the initiation code, it awaits data, checking for data until the specified number of data are received (for the present experiments, 50 data points were captured at each time interval);
- Once the second initiation code is received and verified by the microcontroller, the sensor begins to collect data;
- Each set of data are A/D-converted and modified;
- The data are then sent to the DAQ via serial communication;
- Once the acquisition and transmission of data are complete, the sensor powers down the optical board and returns to sleep mode; and,
- Once the DAQ has received and stored all expected data, it delays for the specified amount of time (1 h for the present experiments), before repeating the process.

The microcontroller code was written in 68HC12 assembly language (Freescale Semiconductor Inc., Austin, Texas), using WinIDE as a compiler.

2.7. Laboratory testing

The objective of the initial laboratory bench test experimental work was to determine the performance characteristics of the sensor under controlled conditions, including the assessment of the different sensor components and housing configurations, and to elucidate the relationship between output voltage data and the degree of mould colonization.

When optimizing the sensor operation, it was first necessary to determine the warm-up time needed before the sensor yielded steady-state data. Secondly, it was necessary to determine the number of replicate data samples needed to ensure an accurate mean value, whilst minimizing the storage demands on the system. Thirdly, the sensor sensitivity needed to be ascertained in order to define how clearly the sensor could discriminate between different amounts of mould growth. Fourthly, the variability between sensors was determined, and the sources of variation evaluated. Lastly, the uniformity of the response within a given sensor was examined. The following laboratory tests were conducted:

2.7.1. Grey-scale testing

Squares representing 8-bit grey-scale values (0–255, black to white) in increments of 50 steps, were prepared in Microsoft PowerPoint, printed at four per sheet on an HP laser jet printer (Model HP1020), and affixed to a flat surface. These test patches were used to determine: 1) the duration of any transient effects in relation to the power-up of the optical components; 2) the number of data points required to achieve a steady-state average output voltage; and, 3) the performance of all the sensors on a common test panel.

2.7.2. LED variability

A glass plate on which a white paper had been affixed to its upper surface was cantilevered on a laboratory bench. A SLR camera was placed on a tripod beneath the glass and aligned below the position of the sensor annulus. Each sensor was positioned on the paper, in turn, with its LED powered on, and a photograph was taken of the illuminated area from beneath the glass. Manual camera settings were used to ensure that the exposure parameters were uniform. Photographs were evaluated using Adobe Photoshop to determine the brightness and uniformity of each sensor LED.

2.7.3. Photodiode variability

The sensor-to-sensor variability of the photodiode response was examined in darkness by occluding each LED with opaque tape to prevent light from reaching the photodiode. Uniform light intensities were then modelled by placing the devices, in turn, on the glass panel (described above) and illuminating them from beneath with a fixed desk lamp. Differing light intensities were simulated by the addition of paper sheets (upto 6) between the glass and the sensor.

2.7.4. Uniformity

In order to determine the uniformity of response of the sensors, a test target was prepared on which a 5.1 mm diameter dot was left

white while the remaining background was black (this configuration was chosen so as not to saturate the photodiode). A number of test targets were generated, again using PowerPoint, with the white dot in different locations. Targets were printed on a laser jet printer, affixed to a flat surface and the sensor placed on top before measurements were taken.

2.7.5. Tuning and sensitivity

Prior to sensor calibration it was necessary to adjust the response of the sensors using grey-scale test targets (described above) and a set of laboratory cultivated test membranes. For comparison, each mould-colonized membrane was also photographed under uniform conditions and settings and the portion of the membrane monitored by the photodiode was then analyzed in Adobe Photoshop to determine the average 8-bit grey-scale pixel intensity.

2.8. Field testing

Once an optimal configuration was determined, 16 sensors were calibrated and installed in two wall panels of the control building at the Insurance Research Lab for Better Homes (IRLBH, London, Ontario, Canada) full-scale field test site [14] to assess their performance in a realistic setting (Fig. 5). In addition to mould sensors, temperature, relative humidity and material moisture content instrumentation were installed in the test panels [15] and connected to the Campbell Scientific CR1000 control and data acquisition system. Two test panels within the control building were instrumented, one with a brick clad exterior and the other with a metal siding exterior.

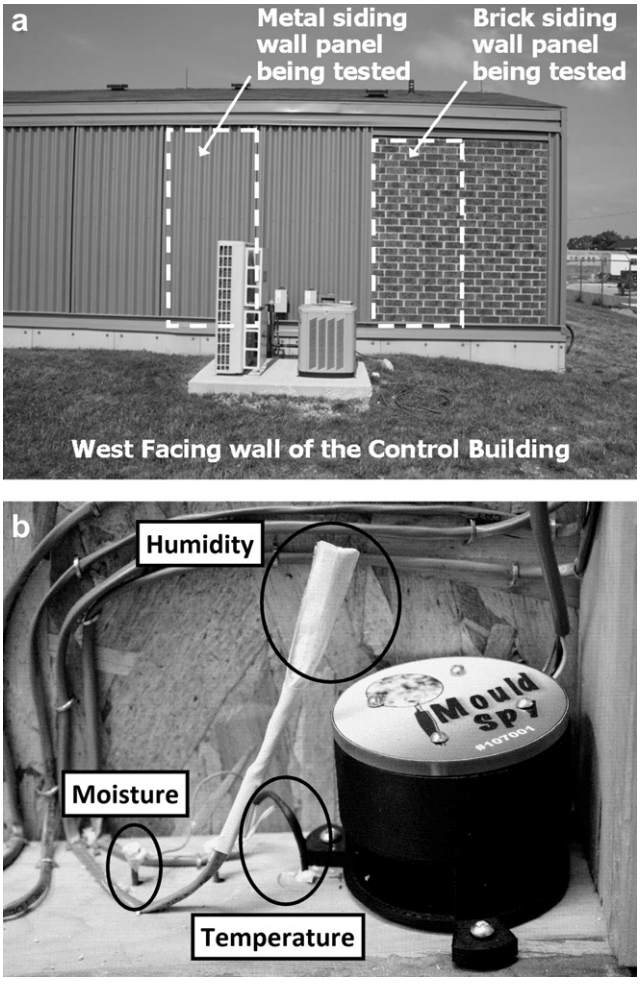

Fig. 5. Illustration of the field installation (a) external view of two instrumented wall panels (b) detail of mould sensor and other environmental sensors (before closing of wall).

3. Results and discussion

3.1. Laboratory testing

3.1.1. Grey-scale testing

A 2 s delay was required after power-on of the optical board in order to achieve a steady response by allowing components to warm-up and the LED to reach its maximum output intensity. The subsequent variation in the data forming the average output voltage was ±2 bit counts (±0.008 V), a typical variation reported in the data sheet for the A/D converter in this microcontroller. It was found that the collection of 50 replicate data points (a 5 s sample) provided a stable average reading whilst minimizing the amount of data storage required and saving battery power. The results of responses of 17 sensors to grey-scale tests are shown in Fig. 6. Most showed saturation at a grey-scale value of 200 possibly due to the glare of the paper. The sensors showed a linear response trend over grey-scale values between 0 and 150, with similar slopes but differing offsets.

3.1.2. LED variability

Illumination of the target area was non-uniform, showing a lateral gradient of varying intensity, due to the location and angle of the LED with respect to the aperture at the base of the sensor. Nevertheless, the minimum, maximum and mean values of the LED illumination were fairly consistent across all sensors (Fig. 7) with the maximum grey-scale difference between any sensors being 29 (sensor 4 = 146, sensor 20 = 175). This consistency suggested that variation in LED output was not responsible for the differences observed in sensor output. Assessment of pixel-to-pixel variation along three parallel transects taken through the illumination images confirmed the gradient to be fairly constant and uniform, with little lateral variation (Fig. 8).

3.1.3. Photodiode variability

In conditions of darkness (LED occluded), each photodiode produced a voltage output of approx. 0.06 V. Using artificial illumination (from below, as described in section 2.7.3), all the sensors generally followed a similar trend (Fig. 9a). Sensors S3 and S4 gave

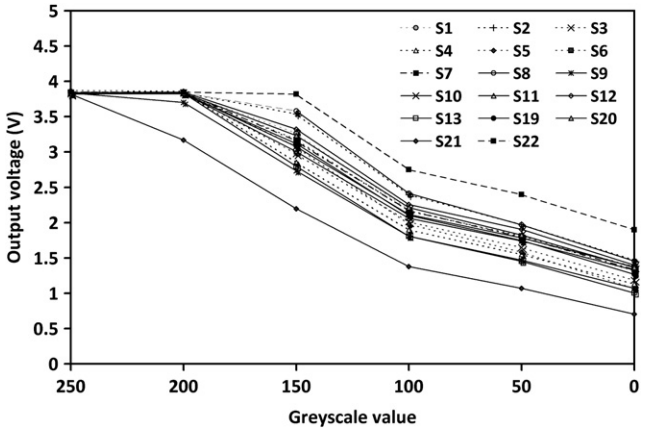

Fig. 6. Grey-scale output voltage readings for all of the tested sensors.

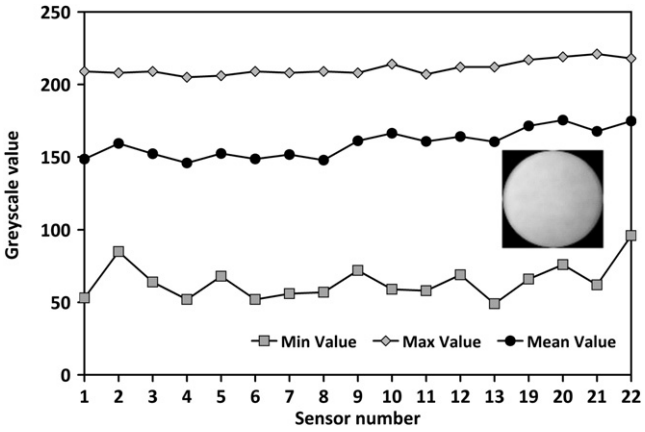

Fig. 7. Mean, minimum, and maximum transmitted LED brightness levels from pixel intensity values (inset: typical example of photographed target).

a much higher output voltage and appeared to saturate at the highest light intensity tested (1 sheet of paper), whilst the output from sensor 7 was slightly lower overall. The photodiode data sheet reported an expected inter-component variability of up to 35% (e.g., 2 V ± 0.7 V) under a common test condition (wavelength of 470 nm at a fixed illumination intensity). Normalizing the data by the unsaturated values (e.g., two sheets of paper) gave a good collapse of the data for most sensors (Fig. 9b). This experiment confirmed that the photodiode was the chief contributor to the observed sensor-to-sensor variation.

3.1.4. Uniformity

Test dots were located at 17 different positions (Fig. 10). All sensors showed the highest output voltages at central dot locations (Fig. 10, light grey region, dot locations 1–5 and 9) whilst the lowest output voltages were observed for dot locations at the periphery of the aperture proximal to the LED (Fig. 10, dark grey region, dot locations 14–16). Differences in magnitudes at any given location were attributed to photodiode variability, as discussed above.

3.1.5. Tuning and sensitivity

The output voltages of the all of the photodiodes became saturated when tested against the least dense grey-scale targets. The majority of data for all sensors fell within the 35% bounds of variability associated with the photodiode response (Fig. 11). The trend

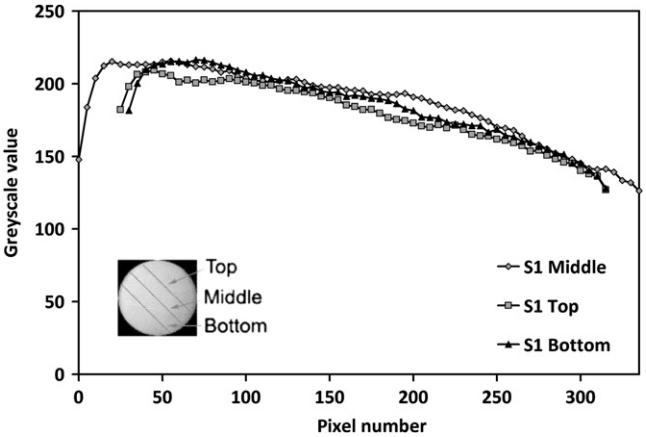

Fig. 8. The LED transmitted grey-scale pixel intensity along the middle, top, and bottom lines through the image for Sensor S1.

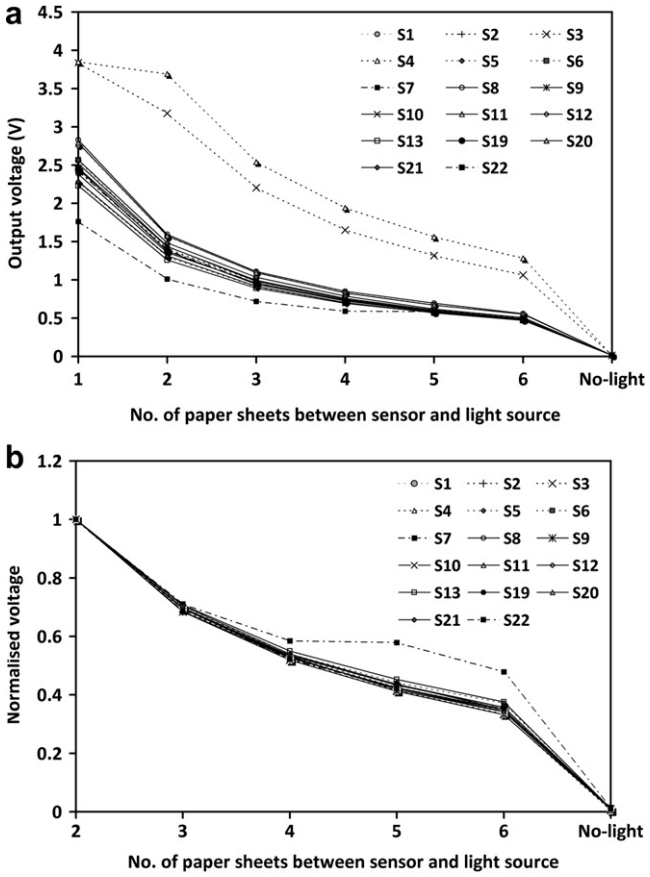

Fig. 9. Photodiode outputs from all the sensors for 7 different light intensities (a) output voltage (b) voltage normalized by second data point (Sheet 2).

in output voltage as a function of mould growth on membranes was similar across all the sensors (Fig. 12), with the sensor-to-sensor variation being associated with a signal gain, rather than an offset. Thus, to ensure a full dynamic range of the optical system, the supply voltage and thus the output intensity of the LED was reduced by the addition of a 169 Ω resistor to the anode of the LED. This resistance value was selected by examining the sensors that natively exhibited the lowest and highest photodiode outputs for a given target.

When normalized to the maximum grey-scale value of 156, the relationship between sensor data and grey-scale values derived from test membrane photographs was a linear function

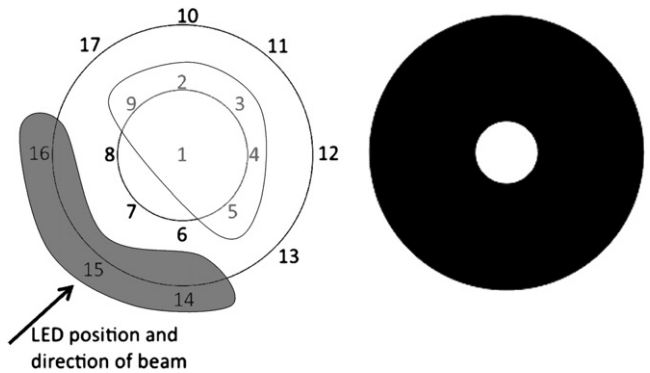

Fig. 10. Uniformity of sensor response, determined from 17 white dot locations, together with a sample of one of the dot targets.

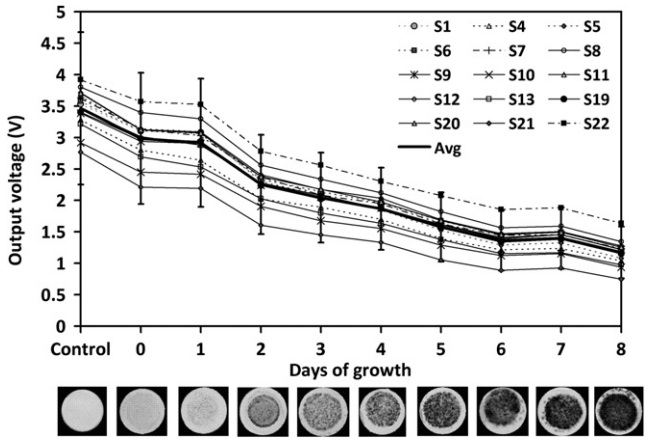

Fig. 11. Output data obtained from the sensors for different days of mould growth.

($R^2 = 0.9887$) (Fig. 13). The dominance of sensor gain with respect to the offset means that whilst each sensor can be subjected to a detailed calibration in the laboratory before being deployed in the field, its subsequent comparative performance may be best evaluated by taking an initial *in situ* value (e.g., baseline reading) and then referencing all subsequent readings to that value.

The average maximum sensor output was 2.29 V (1.17–3.46 V) with a resolution of ±2.5 mV. From the measurements taken on test membranes, ranging from a white (i.e., no mould) to black (i.e., fully colonized), the mould sensor demonstrated a sensitivity of approx. 0.45 grey-scale units mV^{-1} in a manner that was linear across the full range of grey-scale values tested.

3.2. General discussion

Initial results obtained during a 2 month trial period following installation of sensors in the test building have shown the sensors to yield stable voltage data and remain robust in continuous operation (Fig. 14). During this period, no moisture conditions were introduced into the structure, and the sensors performed as expected. The long-term monitoring is continuing and the results will be reported upon conclusion of those experiments.

As part of the laboratory development work the authors have examined a number of questions related to the sensor performance. The first of these is whether it may be used with species of mould other than that examined in the present work. A white LED has been used in order to provide broadband illumination of the membrane and it is possible to utilize photodiodes with different filters on them for different mould species. For quantitative measurements each species would require its own calibration (for example the voltage change with time under fixed temperature and humidity conditions). Since, in the development work reported in this paper, the mould species *C. sphaerospermum* (a heavily melanized brown-black mould with the greatest absorbance in the blue region of the spectrum) was selected, a blue-filtered photodiode was used. The

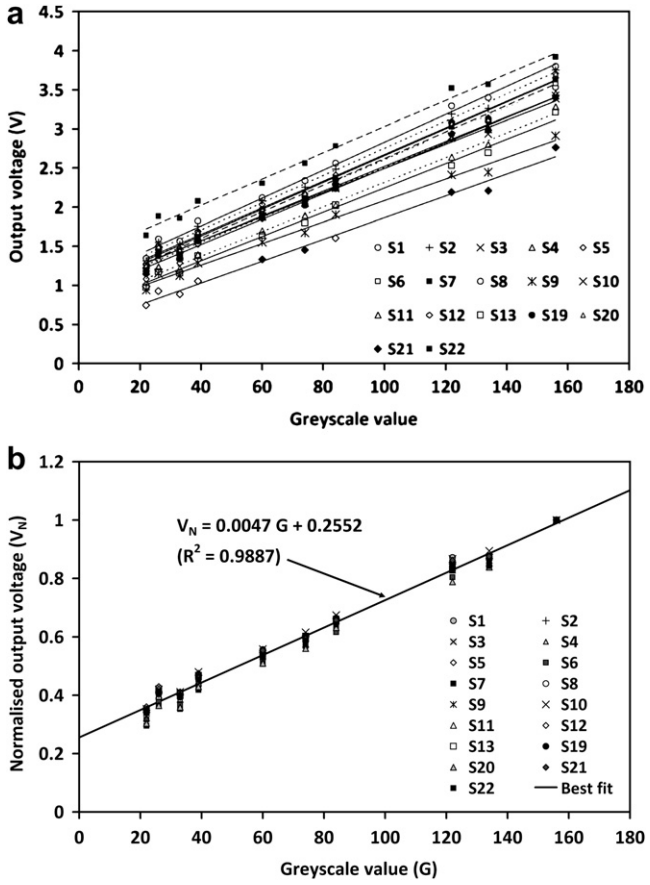

Fig. 13. Sensor output voltages versus photograph grey-scale values across all of the membranes for all of the sensors (a) output voltage (b) voltage normalized by highest grey-scale value for each sensor.

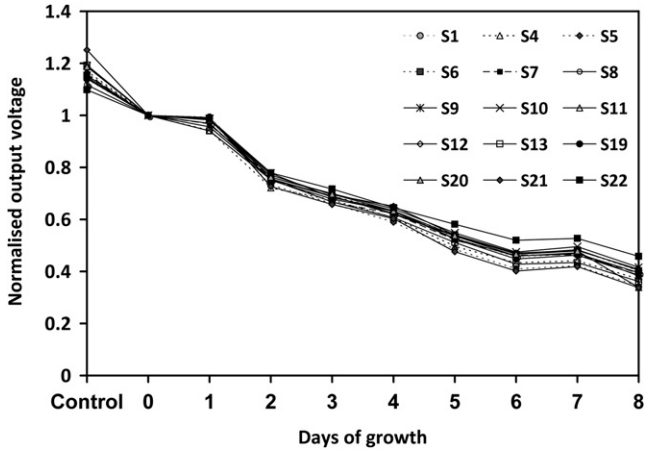

Fig. 12. Output data from the sensors normalized by initial (Day 0 membrane) output.

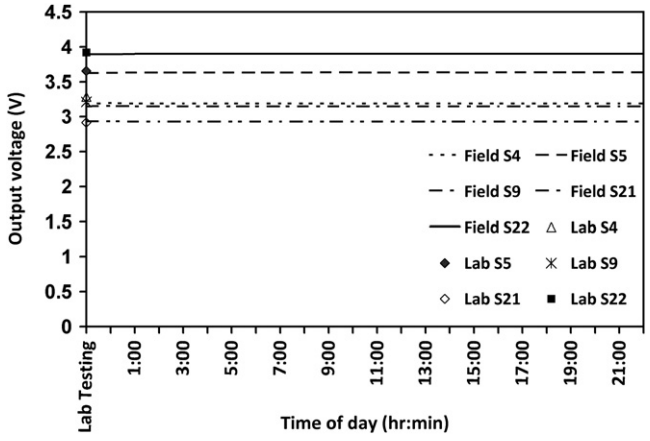

Fig. 14. Comparison of field and laboratory data for some of the sensors.

results shown in Fig. 11 revealed that the voltage change associated with the difference between the reflectance from a membrane with no mould growth and the same membrane fully-covered with mould is about 2 V. Recently, some sensors were modified in order to carry out experiments with a different mould species, *Penicillium verrucosum*, which is blue-green in colour. The same optical components reported in the present paper were used and it was still possible to achieve a voltage range of 1 V, despite the non-optimal photodiode in this application. Hence, the sensor may be readily used for different species, after a laboratory calibration for that species, with the photodiode being changed only if it is found to be necessary to do so in order to achieve a desired voltage range.

The second question is the effect of *in situ* wetting of the membrane, for example due to excessive moisture in a wall cavity. Laboratory experiments have shown that the voltage changes associated with any change in reflectance due to wetting of the membrane are relatively small and the voltage remains within 0.2 V of its initial value if the membrane dries out again, in the absence of any mould growth, which may be compared with the, much larger, approximately 2 V change associated with the change from no mould growth to a membrane fully-covered with mould. The effect of wetting also has a much more rapid variation with time when compared to the gradual, monotonic decrease in voltage as mould grows on the membrane.

Finally, there is the question of dust and debris falling onto the membrane surface. The experiments have shown that the voltage time history associated with particle deposition on the membrane, together with the subsequent movement and removal of those particles (especially under the action of gravity when the sensor is mounted on a vertical surface, for example a building wall), is very different from that associated with mould growth. The voltage changes due to the former are sudden, being a small jump from one data point to the next (over, say, 15 min), whereas voltage changes due to mould growth are smooth and gradual, occurring over many days and over many data points. Thus, it is possible to distinguish between the two effects.

4. Conclusions

A new, optoelectronic mould sensor has been developed and optimized, with its performance, notably the sensor-to-sensor variation, quantified and understood through an extensive series of laboratory bench-tests. The voltage outputs from the sensors have been shown to be very sensitive to different amounts of mould growth on the sensor's active element, a mould-inoculated membrane. The output trends were found to be identical for all of the sensors built and tested, with the difference in magnitude from one sensor to another being in gain only and mostly attributable to the inherent variability in sensitivity from one photodiode to another.

The underlying principle of the sensor is that the substrate over which mould grows becomes modified in its spectral reflective characteristics. This modification is both a function of the development of pigments in the mycelium and spore mass as well as textural differences between the colony surface and the uncolonized substrate. The measurement of these changes with a light source and detector may be used to monitor the growth of mould on a specific area of a building material surface. Mould growth may be quantified either by a measurement of mould biomass as a function of reflected light intensity or, more simply from laboratory tests, by calibrating the reflected light intensity against patterns of mould growth observed after a given number of days exposure under controlled environmental conditions.

A total of 16 sensors have been installed in two wall assemblies of a test building and their long-term performance is presently being monitored, supported by data from other adjacent environmental sensors. In addition, a wireless version of the sensor is being developed as an installable upgrade to the existing devices, in order to achieve a fully remote sensor for detecting the onset of hidden mould growth.

It is anticipated that development of this instrumentation platform to monitor actual mould growth, in addition to existing technology that can be used to measure temperature, relative humidity, moisture content and air movement, will facilitate the controlled study of the performance of construction designs with respect to moisture and biological contaminants, and contribute to the development of evidence-based practices in building design and construction.

Acknowledgements

This research was assisted by undergraduate students T Chan, K Groen, M Eng, and V Wong. Thanks are also due to M Al-Naama, at the University of Toronto for growing the mould membranes and E Porter and D Phillips from The University of Western Ontario's electronic and machine shops for their advice and help. The authors are grateful to the Canadian Foundation for innovation (CFI), the Natural Sciences and Engineering Research Council of Canada (NSERC), the Ontario Innovation Trust (OIT), the Insurance Bureau of Canada and an anonymous industry donor for their financial contributions to the project, without which this research would not have been possible. This manuscript was written whilst E Savory was supported by a Region Pays de la Loire Visiting International Researcher position at the Ecole Centrale de Nantes, France.

References

[1] Abe K. A method for numerical characterization of indoor climates by a biosensor using a xerophilic fungus. Indoor Air 1993;3:344–8.
[2] Tobin RS, Baranowski E, Gilman A, Kuiper-Goodman T, Miller JD, Giddings M. Significance of fungi in indoor air: report from a working group. Can J Public Health 1987;78:S1–30.
[3] Krieger J, Jacobs DE, Ashley PJ, Baeder A, Chew GL, Dearborn D, et al. Housing interventions and control of asthma-related indoor biologic agents: a review of the evidence. J Publ Health Manag Pract 2010;16:S11–20.
[4] Institute of Medicine. Clearing the air: asthma and indoor air exposures. Washington, D.C.: National Academies Press; 2000.
[5] Institute of Medicine. Damp indoor spaces and health. Washington, D.C.: National Academies Press; 2004.
[6] Flannigan B, Samson RA, Miller JD, editors. Microorganisms in home and indoor work environments. Diversity, health impacts, investigation and control. 2nd ed. Taylor & Francis; 2011.
[7] Adan OCG, Samson RA. Fundamentals of mold growth in indoor environments and strategies for healthy living. 1st ed. The Netherlands: Wageningen Academic; 2011.
[8] De Jesus VR, Balasubramanian G, Bayer CW, Greneker GF, Harriman LG, Hendry RJ, et al. Portable mold sensors: technical feasibility and operational requirements. Georgia Tech Research Institute; March 2006. Final Report ARTI-21CR/612-40080-03.
[9] Abe K, Nagao Y, Nakada T, Sakuma S. Assessment of indoor climate in an apartment by use of a fungal index. Appl Environ Microbiol 1996;62:959–63.
[10] Abe K, Kawakami Y, Hamano T, Imai Y, Iso K. Measured fungal index determined using fungal growth and computed fungal index based on temperature and relative humidity in houses. In: Proc 6th Int conf on indoor air quality, ventilation and energy conservation in buildings, vol. 1; 2007. p. 296–301.
[11] Sauer A, Scott J, Savory E, Sabarinathan J. Mould spy – the design and evaluation of a photoelectronic mould sensor. In: Proc Can Soc Mech Eng (CSME) Forum 2008, Ottawa, June 2008 [on CD-ROM].
[12] De Hoog GS, Queiroz-Telles F, Haase G, Fernandez-Zeppenfeldt G, Angelis DA, van den Ende A, et al. Black fungi: clinical and pathogenic approaches. Med Mycol 2000;38:243–50.
[13] Malloch D. Moulds: their isolation, cultivation and identification. Toronto, Ontario: University of Toronto Press; 1981.
[14] Bartlett FM, Galsworthy JK, Henderson D, Hong HP, Iizumi E, Inculet DR, et al. The three little pigs project: a new test facility for full-scale small buildings. In: Proc 12th Int conf on wind engineering, Cairns, Australia, July, 2007 [on CD-ROM].
[15] Straube J, Onysko DM, Schumacher C. Methodology and design of field experiments for monitoring the hygrothermal performance of wood frame enclosures. J Therm Envelope Build Sci 2002;26:123–50.